

Reduced-Order Modeling for PDEs with bifurcating solutions: applications in CFD

Annalisa Quaini

Department of Mathematics, University of Houston



Joint work with: M. Hess, G. Pitton, G. Rozza (SISSA, Italy),
A. Alla (PUC-Rio), M. Gunzburger (FSU).

Acknowledgements: NSF DMS-1620384.

Algorithms for Dimension and Complexity Reduction
ICERM, March 23-27, 2020

Bifurcation in physical systems

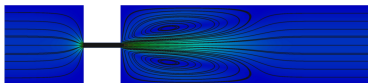
Many physical systems show a sudden change in behavior as one or more parameters are varied in a smooth way.

Examples:

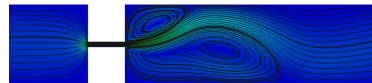
- Incompressible flow in a contraction-expansion channel

Parameter: Reynolds number

below a critical value



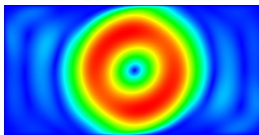
above a critical value



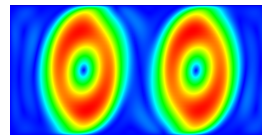
- Rayleigh-Bénard cavity

Parameter: Grashof number

below a critical value



above a critical value



This kind of behavior is studied in **bifurcation theory**.

[Ambrosetti-Prodi, *Cambridge University Press* 1993]

Why do some problems have bifurcating solutions?

We consider a problem that depends on a point $\mu \in \mathbb{R}^n$ in the parameter domain.

Given $\mu \in \mathbb{R}^n$, find $u \in X$ such that

$$F(\mu, u(\mu)) = 0$$

$$F : \mathbb{R}^n \times X \rightarrow Y$$

with X, Y Banach spaces.

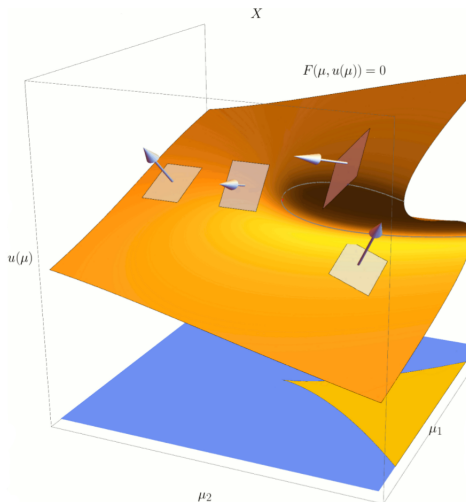
Example: $F(\mu, u(\mu)) = \mu \mathcal{L}u + \mathcal{N}(u)$ and $Y = X$.

The nonlinearity $\mathcal{N}(u)$ can produce a **loss of uniqueness** for u and introduce multiple branches of solutions in some parameter range.

When multiple solutions branch from a known solution, we say that a **bifurcation point** has occurred.

Critical bifurcation points

$F(\mu, u(\mu)) = 0$ defines a manifold in the ambient space.



At a critical bifurcation point, the surface gradient $D_u F$ is zero.

Model

We use the **incompressible** Navier-Stokes equations as a concrete setting:

$$\begin{aligned} \frac{\partial \mathbf{u}}{\partial t} + \mathbf{u} \cdot \nabla \mathbf{u} - \nabla \cdot \boldsymbol{\sigma} &= \mathbf{f} & \text{in } \Omega \times (0, T) \\ \nabla \cdot \mathbf{u} &= 0 & \text{in } \Omega \times (0, T) \end{aligned}$$

\mathbf{u} : fluid velocity

$\boldsymbol{\sigma} = -p\mathbf{I} + 2\nu\boldsymbol{\varepsilon}(\mathbf{u})$: Cauchy stress tensor

p : fluid pressure

$\boldsymbol{\varepsilon}(\mathbf{u}) = \frac{(\nabla \mathbf{u}) + (\nabla \mathbf{u})^T}{2}$: strain rate tensor

We are interested in **steady state solutions**, obtained by either time-advancement or fixed-point iterations.

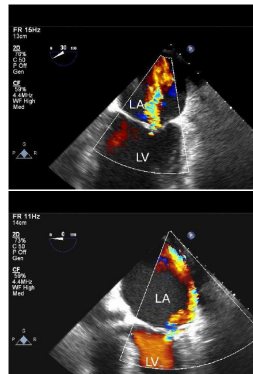
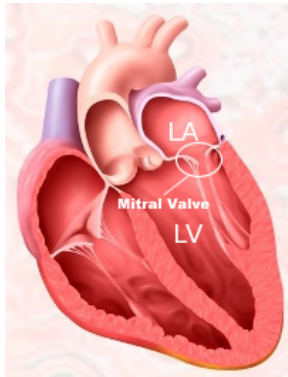
The software framework **Nektar++**¹ is used for the full order simulations. Nektar session files are released within C++ **ITHACA-SEM** framework².

¹<https://www.nektar.info/>

²<https://github.com/mathLab/ITHACA-SEM>

Application 1: mitral regurgitant flow

Mitral valve Regurgitation is a valvular heart disease associated with the abnormal leaking of blood from the left ventricle into the left atrium of the heart.



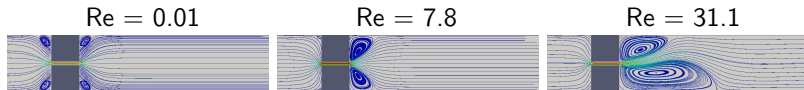
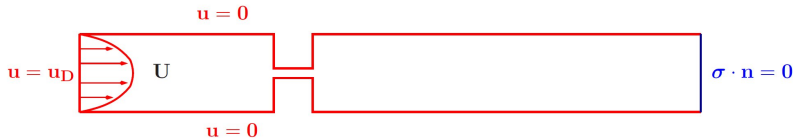
central jet

Coanda jet

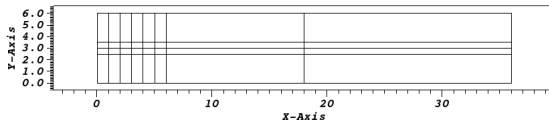
Accurate echocardiographic assessment of the volume of blood that regurgitates is an ongoing challenge, in particular in presence of the Coanda effect.

Jet flow

Let us simplify the geometry and understand under which conditions trigger the Coanda effect. Let $Re = Uw/\nu$ and $\mathbf{f} = \mathbf{0}$.

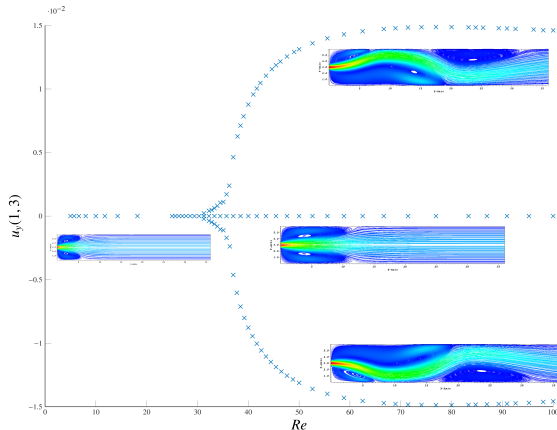


We partition the domain into [spectral elements](#), with a total of 14259 degrees of freedom using modal Legendre ansatz functions of order 12.



Bifurcation for the jet flow

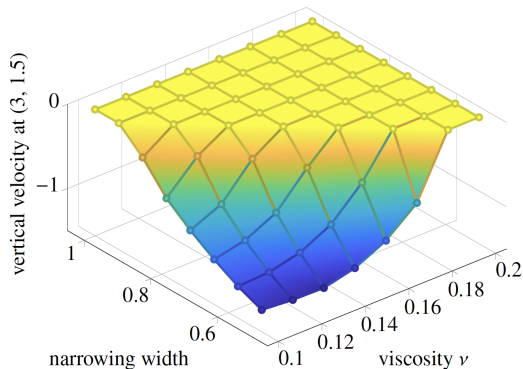
Symmetry breaking bifurcation (Coanda effect) in a 2D channel with expansion ratio 1:6. Vertical velocity is taken on the horizontal axis, at distance 1 from the inlet. We can also vary the narrowing width.



[Pitton-Q-Rozza, *JCP* 2017] [Drikakis, *Phys. Fluids* 1997]

Bifurcation for the jet flow - 2 parameters

Symmetry breaking bifurcation in a 2D channel with **variable kinematic viscosity** ν and **variable narrowing width**. Vertical velocity is taken on the horizontal axis, at distance 1.5 from the inlet.



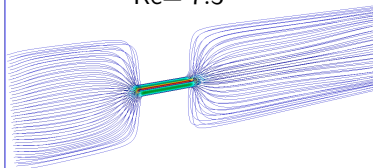
The graph shows the stable lower branch.

[Hess-Q-Rozza, *arXiv:1812.11051* 2018, accepted in ICOSAHOM 2018 proceeding]

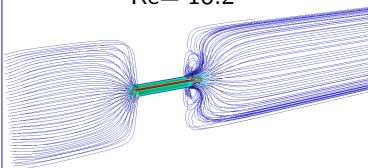
Jet flow: another possible parameter

3D channel with expansion ratio 1:15.4 and aspect ratio 3/2.

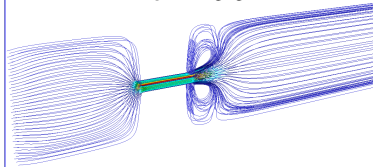
Re= 7.3



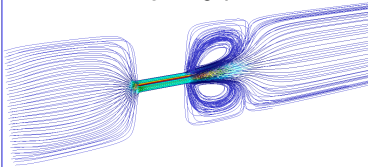
Re= 18.2



Re = 25.5

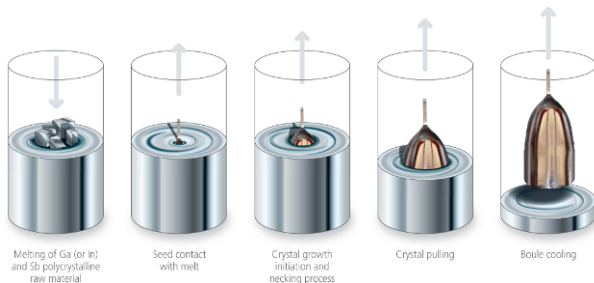


Re= 43.7



Application 2: semiconductor crystal growth

Under rotation and simultaneous pulling of the seed, the melt of high-purity silicon crystallizes and a **mono-crystalline rod** develops.



The Rayleigh-Bénard **instability in the melt is increasingly difficult to suppress** by crucible/crystal rotation as the melt height is increased.

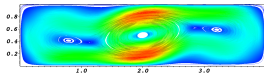
We consider a simplified problem: a Rayleigh-Bénard cavity.

Rayleigh-Bénard cavity

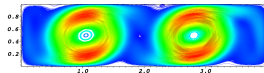
- Rectangular cavity with height 1 and length A .
- Left wall maintained at temperature T_0 .
- Right wall maintained at temperature $T_0 + \Delta T$.
- Horizontal walls are thermally insulated.

We set Prandtl number $Pr = 0$. Let $Gr = \frac{g\beta\Delta T}{A\nu^2}$ and $\mathbf{f} = (0, Gr\nu^2x)^T$.

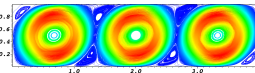
$Gr = 20 \cdot 10^3$



$Gr = 40 \cdot 10^3$



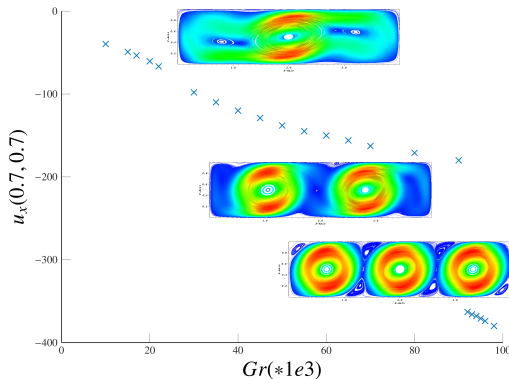
$Gr = 98 \cdot 10^3$



We partition the domain into [spectral elements](#), with a total of 6321 degrees of freedom using modal Legendre ansatz functions of order 16.

Bifurcation for the cavity

Bifurcation diagram for the Rayleigh-Bénard cavity with aspect ratio 4. Horizontal velocity component is taken at point $(0.7, 0.7)$.



Discontinuities are around $Gr = 25 \cdot 10^3$ and $Gr = 90 \cdot 10^3$.

[Pitton-Rozza, *J Sci. Comput.* 2017] [Gelfgat et al., *J. Fluid Mech.* 1999]

[Herrero-Maday-Pla, *CMAME* 2013]

Suited for Reduced-Order Modeling

- To plot the bifurcation diagram for a given geometric configuration, the simulations associated to **several parameter values** (e.g., Re or Gr) have to be run.
- Each flow simulation is **computationally expensive**.
- Simulations become even more computationally expensive when the flow parameters are near the critical value for a bifurcation.

We propose:

1. A **global Reduced-Order Modeling (ROM)** approach, that does not respect the large differences in the solutions corresponding to different subregions.
[Pitton-Q-Rozza, *JCP* 2017]
2. A **local ROM** approach specifically aimed at bifurcation problems.
[Hess-Alla-Q-Rozza-Gunzburger, *CMAME* 2019]

Global ROM: Approximation stability

We use **Proper Orthogonal Decomposition (POD)** to compute a set of orthogonal basis functions $\{\varphi_i\}_{i=1}^N$ from the velocity snapshots. Same procedure can be applied to the pressure snapshots.

The **Reduced Basis** spaces:

$$\mathbf{V}^N = \text{span}\{\varphi_i, i = 1, \dots, N\}$$

$$Q^N = \text{span}\{\sigma_i, i = 1, \dots, N\}$$

are not guaranteed to fulfill a parametrized **inf-sup** condition

$$\inf_{q \in Q^N} \sup_{\mathbf{v} \in \mathbf{V}^N} \frac{\int_{\Omega} q \nabla \cdot \mathbf{v} d\Omega}{\|q\|_{Q^N} \|\mathbf{v}\|_{\mathbf{V}^N}} = \beta^N > 0,$$

Approximation stability can be achieved through:

- supremizer enrichment of the velocity space [Rozza, Veroy, *CNAME* 2007];
- Petrov-Galerkin projection during online phase [Amsallem, Farhat, *IJNME* 2012], [Dahmen, 2015];
- **Piola transformation** [Lovgren et al, *ESAIM* 2006].

Piola transformation

The Piola transformation consists in an **online processing** of the velocity basis set $\{\varphi_i\}$ that allows to obtain a set of weakly **divergence-free basis functions** $\{\varphi_i^{\text{div}}\}$:

$$\mathbf{u}^N(\mu) = \sum_{i=1}^N u_i^N(\mu) \varphi_i^{\text{div}}$$

Two possibilities to recover the pressure:

- use the velocity coefficients:

$$p^N(\mu) = \sum_{i=1}^N u_i^N(\mu) \sigma_i$$

- solve a Poisson problem (online):

$$\Delta p^N(\mu) = -\nabla \cdot (\mathbf{u}^N(\mu) \cdot \nabla \mathbf{u}^N(\mu))$$

Global ROM for jet flow

The symmetry breaking bifurcation (Coanda effect) is a **supercritical pitchfork bifurcations**.

To detect numerically the presence of these bifurcation points, we rely on the **spectrum analysis** of linearized operator:

$$\mathcal{L}(\mathbf{u}^N(\mu))[\varphi_i^{\text{div}}] = \mathbf{u}^N(\mu) \cdot \nabla \varphi_i^{\text{div}} + \varphi_i^{\text{div}} \cdot \nabla \mathbf{u}^N(\mu).$$

At a pitchfork bifurcation point, a **simple eigenvalue of \mathcal{L} changes sign**.

To make sure that the approximation is lying on the correct branch we use a **continuation method**.

Other techniques would have to be used for different kind of singular points (e.g., Hopf bifurcations) occurring at higher Reynolds numbers or in different settings.

[Ambrosetti-Prodi, *Cambridge University Press* 1193] [Cliffe-Spence-Tavener, *Acta Numerica* 2000] [Dijkstra et al., *CoCP* 2014]

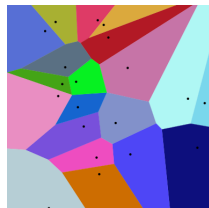
Local ROM: K-means clustering of snapshots

Idea: cluster the snapshots to construct several **local bases**, each of which is used for parameters belonging to a different subregion of the bifurcation diagram.

K-means clustering: given a discrete set of vectors $\mathcal{Y} = \{\mathbf{y}_1, \dots, \mathbf{y}_M\}$ in \mathbb{R}^n , it computes a partitioning of \mathcal{Y} into K clusters \mathcal{V}_k .

[Du-Faber-Gunzburger, *SIAM review*, 1999].

Cluster (or Voronoi region) \mathcal{V}_k with generator \mathbf{z}_k :



$$\mathcal{V}_k = \{\mathbf{y} \in \mathcal{Y} : d_p(\mathbf{y}, \mathbf{z}_k) \leq d_p(\mathbf{y}, \mathbf{z}_i), \text{ for } i = 1, \dots, K \text{ and } i \neq k\}.$$

The snapshot set is \mathcal{Y} and $d_p(\mathbf{v}, \mathbf{w}) = \|\mathbf{v} - \mathbf{w}\|_{L_2}^2$ in the discrete L_2 norm.

K-means algorithm

Define **k-means energy** \mathcal{F} as

$$\mathcal{F}(\mathbf{z}_1, \dots, \mathbf{z}_K; \mathcal{V}_1, \dots, \mathcal{V}_K) = \sum_{k=1}^K \sum_{\mathbf{y} \in \mathcal{V}_K} d_p(\mathbf{y}, \mathbf{z}_k).$$

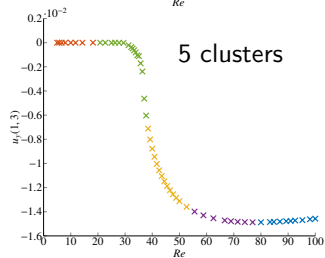
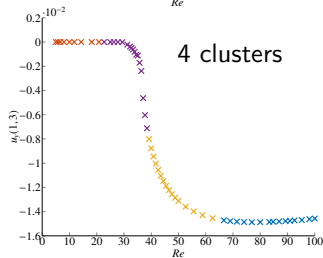
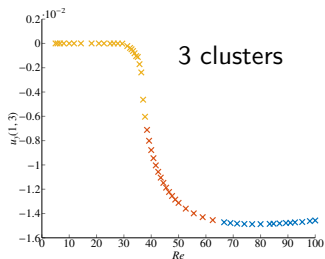
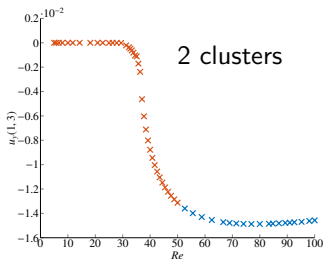
Input: snapshot set $\mathcal{Y} = \{\mathbf{y}_1, \dots, \mathbf{y}_M\}$ and number of clusters K

- Step 0: randomly choose K vectors from \mathcal{Y} as generators \mathbf{z}_k
- Step 1: find closest generator for each $\mathbf{y}_i \in \mathcal{Y}$
- Step 2: define Voronoi region \mathcal{V}_k as the set of \mathbf{y}_i closer to \mathbf{z}_k
- Step 3: assign new generators \mathbf{z}_k as the mean of all vectors in \mathcal{V}_k
- repeat Step 1, 2, 3 until the k-means energy does not decrease “significantly”

Output: Voronoi regions \mathcal{V}_k and k-means energy

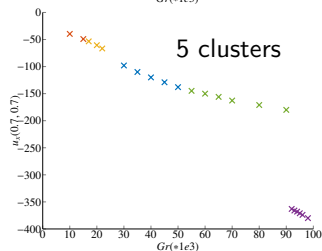
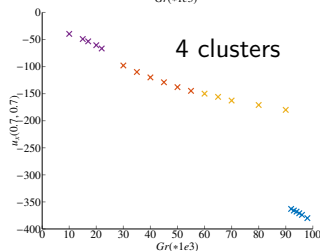
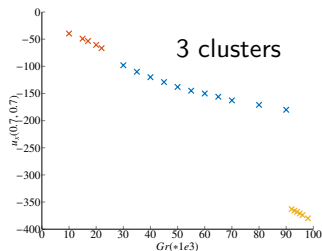
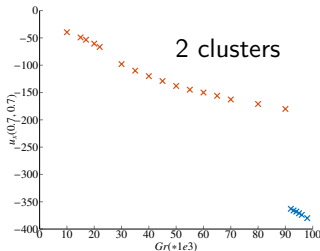
Jet flow: clustering results

Lower branch of the bifurcation diagram and k-means clustering of snapshots for 2, 3, 4, and 5 clusters.



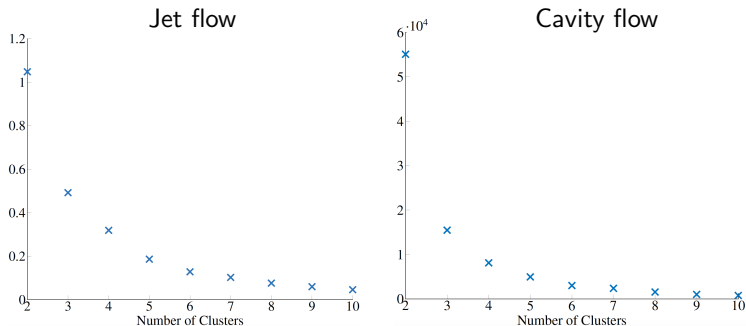
Cavity flow: clustering results

Bifurcation diagram and k-means clustering of snapshots for 2, 3, 4, and 5 clusters.



K-means energies

K-means energy vs the number of clusters K for both problems.



For $K > 5$, the k-means energy decreases at each step by roughly 15%, so no “elbowing” effect occurs. Nonetheless, for $K > 5$ we have a gentle slope. That is why we stopped at $K = 5$.

Local ROM: POD sampling

Each local ROM basis is meant to help account for a **separate subregion of the parameter domain**, including those that straddle across the boundaries between two subregions of the bifurcation diagram.

To construct the local ROM bases, we use **Proper Orthogonal Decomposition**. For each cluster L , we compute local ROM V_L .

Let A be the linearized Navier-Stokes element matrix. The steady-state ROM solution is computed by fixed point iteration scheme, solving at each step:

$$V_L^T A V_L \mathbf{x}_r = V_L^T \mathbf{b}.$$

The re-projected ROM solution is:

$$\mathbf{x} = V_L^T \mathbf{x}_r.$$

[Lassila et al., *Springer* 2014]

Global ROM for jet flow: one parameter study

To plot the bifurcation diagram for the symmetry breaking for the channel with expansion ratio 1:6, we take $N = 9$ basis functions and run 80 simulations.

Computational time for one simulation with

- full order model: **10 CPU hours**
- reduced order model: **few seconds**

Estimation of the computational cost reduction:

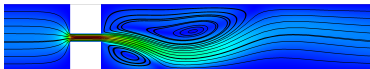
$$\frac{\text{Time to build the RB spaces} + \text{Online time to detect the bifurcation point}}{\text{Time of the equivalent full order computation}}$$

$$= \frac{9 \cdot 10h + 2h + 0.08h}{80 \cdot 10h} \simeq \mathbf{11.5\%}.$$

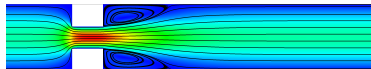
Global ROM for jet flow: two parameter study

Variable expansion ratio λ and Reynolds number:

Re= 40, expansion ratio 1 : 8

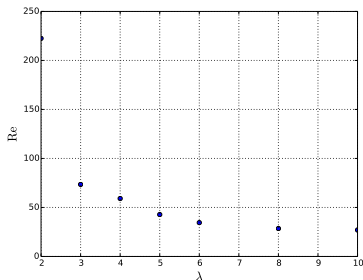


Re= 45, expansion ratio 1 : 3



The critical Reynolds number for the symmetry breaking decreases as the expansion ratio increases.

In particular, we see that it decreases fast for small values of the expansion ratio.



Here $N = 42$ and the estimated computational cost reduction is:

$$\frac{42 \cdot 10h + 2h + 7 \cdot 0.08h}{7 \cdot 10h \cdot 80} \simeq \mathbf{7.5\%}.$$

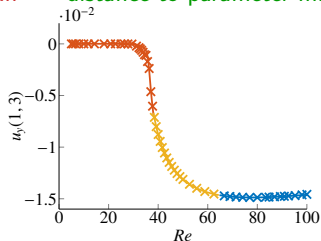
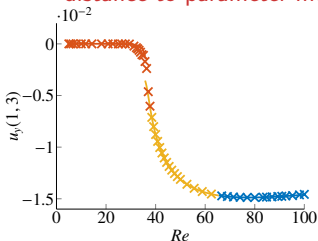
Jet: assignment of local ROM basis

Bifurcation diagrams and assignments of parameters to local ROMs using two criteria for the assignment of the local ROM bases.

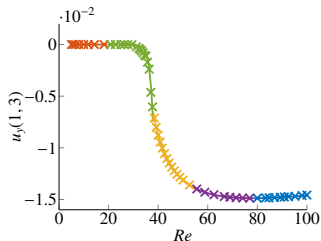
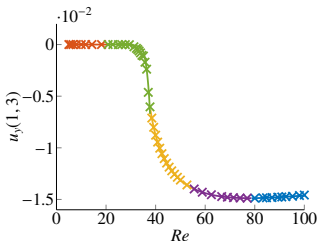
distance to parameter mean

distance to parameter mid-range

3 clusters



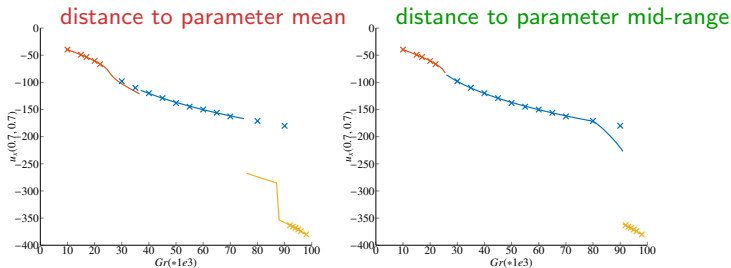
5 clusters



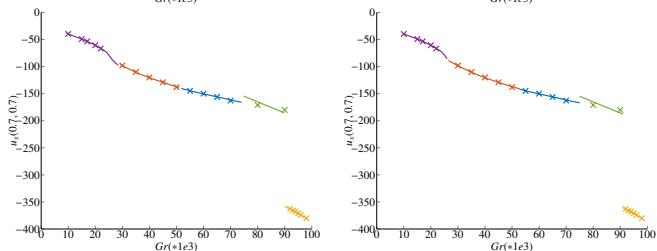
Cavity: assignment of local ROM basis

Bifurcation diagrams and assignments of parameters to local ROMs using two criteria for the assignment of the local ROM bases.

3 clusters



5 clusters



local ROM vs global ROM

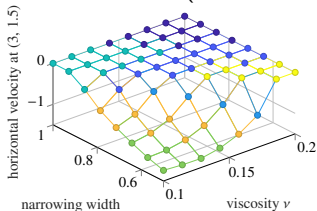
Comparison at 10 (jet) and 5 (cavity) uniformly sampled parameter locations, which were not part of the training grid.

- In average, our local ROM shows improved accuracy over our global ROM.
- Our local ROM provides accurate results over the whole parameter range with the **distance to parameter mid-range**.
- Using **distance to parameter centroid**, our local ROM become inaccurate at the switching point between local bases.
- **Jet**: a global ROM fails for higher Re.
- **Cavity**: a global ROM fails close to the discontinuous bifurcation points.
- **Cavity**: the clustering algorithm has identified parameter ranges where snapshot solutions are similar, i.e. solutions of 1,2 and 3 rolls are separated from each other.

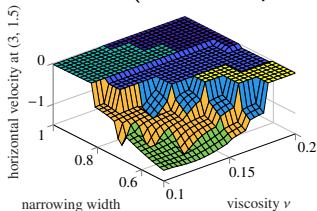
Local ROM: Bifurcation for the jet flow - 2 parameters

Stable lower branch of the symmetry breaking bifurcation in a 2D channel with variable kinematic viscosity ν and variable narrowing width. Vertical velocity is taken on the horizontal axis, at distance 1.5 from the inlet.

Full order model (with clustering)



Local ROM (closest snapshot)



The geometric affine transformations are introduced in [Hess-Q-Rozza, *arXiv:1812.11051* 2018, accepted in ICOSAHOM 2018 proceeding]. A curved geometry is considered in [Hess-Q-Rozza, *IJCFD* 2019] and the reduction uses the empirical interpolation method.

Conclusions

- For 2 academic problems our local ROM proves to be **more accurate than a global ROM**.
- We used a **k-means clustering of snapshots** as the starting point for constructing a local ROM.
- We gave a **recipe for detecting which local basis to use** for any given parameter point not used to determine the snapshots.
- We accounted for the differences between **bifurcations that cause continuous (jet) or discontinuous (cavity) changes** in the solution.

THANK YOU FOR YOUR ATTENTION!



<https://github.com/mathLab/ITHACA-SEM>

[Pitton-Q-Rozza, *JCP* 2017]

[Hess-Alla-Q-Rozza-Gunzburger, *CMAME* 2019]